OTFS-IDMA: An Unsourced Multiple Access Scheme for Doubly-Dispersive Channels

Davide Bergamasco, Federico Clazzer, and Paolo Casari

***Abstract*—We present an unsourced multiple access (UMAC) scheme tailored to high-mobility wireless channels. The proposed construction is based on orthogonal time frequency space (OTFS) modulation and sparse interleaver division multiple access (IDMA) in the delay-Doppler (DD) domain. The receiver runs a compressive-sensing joint activity-detection and channel estimation process followed by a single-user decoder which harnesses multipath diversity via the maximal-ratio combining (MRC) principle. Numerical results show the potential of DD-based uncoordinated schemes in the presence of double selectivity, while remarking the design tradeoffs and remaining challenges introduced by the proposed design.**

***Index Terms*—Delay-Doppler; doubly-selective; high-mobility; random-access; interference cancellation; polar codes; maximal-ratio combining; approximate message passing**

I. Introduction

Internet of Things (IoT) applications are often characterized by a large number of devices aiming to report short and sporadic messages to a common receiver [1]. Distributed transmitters may be difficult to coordinate without incurring large system overhead or unbearable delays, especially in settings with a massive amount of transmitting nodes. Considering these issues, an appealing alternative is given by grant-free multiple access (MAC) schemes.

Grant-free MAC strategies have been extensively studied in the past in the context of random access (RA) [2]. The recent introduction of the unsourced multiple access (UMAC) framework [3] provided an achievability bound on the energy efficiency for uncoordinated MAC schemes. It also proved that recent RA solutions are not optimal. Hence, the research community has tackled the problem and proposed several new protocols, e.g. [4]–[8], that are closing the gap with the random-coding performance provided in [3]. The initial analysis of the UMAC was carried out assuming a Gaussian multiple access channel (GMAC). Successive research extended the bound and developed practical protocols for the quasi-static Rayleigh fading channel [7], [9], where the signal of each user is received with a different channel gain.

D. Bergamasco and F. Clazzer are with the Inst. of Communications and Navigation, German Aerospace Center (DLR), Wessling, Germany (e-mail: {davide.bergamasco, federico.clazzer}@dlr.de), and would like to thank the Federal Ministry of Research, Technology, and Space (BMFTR) for supporting the xG-RIC project as part of the research program Communication Systems "Souverän. Digital. Vernetzt." (grant number 16KIS2429K).

P. Casari is with DISI, University of Trento, Italy (e-mail: paolo.casari@unitn.it), and was partally supported by the European Union – Next Generation EU – PNRR, Mission 4 Component 2, Investment 1.3 – PE RESTART Spoke 6 - Project EMBRACE (PE00000001, CUP E63C22002070006).

In this paper, we considered the channel to be doubly-dispersive, as is typical in high-mobility settings. Relevant examples are vehicular networks or multi-user services relying on low-Earth orbit (LEO) constellations. In satellite-enabled IoT systems, a similar channel representation, characterized by residual time-frequency offsets, holds true when users are not able to perfectly compensate for the Doppler distortion and for the transmission delay due to imprecise information about the satellite trajectory or their own location.

Doubly-dispersive channels introduce strong distortions on the transmitted signals, forcing the receiver to counteract these impairments via equalization in order to retrieve the transmitted messages. It is worth noting that the commonly adopted single-tap equalization of orthogonal frequency-division multiplexing (OFDM) signals is not effective. Large subcarrier spacing helps reduce the performance degradation due to inter-carrier interference (ICI) at the price of lower spectral efficiency, as the relative overhead from the cyclic prefix (CP) becomes more significant. Additionally, to enable reliable equalization, the receiver needs to keep an up-to-date channel estimate. Its time validity is limited due to the short coherence time, thus requiring high pilot overhead. In [10], a scheme based on massive MIMO is proposed to deal with these challenges. In this work, we take a different approach by considering the delay-Doppler (DD) representation of the channel, which shows longer time stability and, in many practical scenarios, can be effectively characterized by a few parameters (see [11]–[14] for a more comprehensive discussion). A convenient way of exploiting the DD channel representation is to embed the information directly in the same domain using, e.g., orthogonal time frequency space (OTFS) modulation [15].

OTFS has been investigated in the general context of random access in [16] and [17] while DD-based activity detection has been studied in [18], [19]. By way of contrast, the main contribution of this paper is to develop a full UMAC scheme that employs OTFS to cope with doubly-dispersive channels. Different from previous DD-based contributions, that focus on the design of the activity detection mechanisms, we develop and merge a second protocol step that enables the detection and decoding of the uncoordinated users messages. To achieve competitive performance, we expand some key ideas developed in the context of grant-free schemes for the GMAC and adapt them to OTFS modulation as well as to the additional challenges introduced by the doubly-dispersive model. Our implementation takes advantage from the principles of sparse interleaver division multiple access (IDMA) and on-off division multiple access (ODMA) derived in [6]

and [7] respectively, where we adapted both the transmitter and receiver operations to work in the DD domain over time-frequency selective channels. We remark the similarities between the IDMA and ODMA strategies. IDMA has been originally introduced in [20], while its application to the UMAC setting has been adopted in [6] and more recently in [21].

The rest of the paper is organized as follows: In Section II we describe the UMAC problem, the considered channel model, and the transmitter/receiver architectures. In Section III we present numerical results on the performance of the proposed scheme, and we discuss design choices toghether with the role of the main parameters. Finally, in Section IV we draw conclusions and propose future directions.

II. System model

We consider a multi-user random access system, where K denotes the total number of users and K_a the subset of active ones. Each of the K_a nodes transmits a b bits message, mapped into n complex channel uses through a common codebook $\mathcal{C}$. Every codeword $\boldsymbol{x}_k \in \mathcal{C} \subset \mathbb{C}^n$ fulfills the power constraint $||\boldsymbol{x}_k||_2^2 \leq nP$. We consider a doubly-dispersive channel model, where the received signal $\boldsymbol{y}(t)$ takes the form:

$$\boldsymbol{y}(t) = \sum_{k=1}^{K_a} \sum_{p=1}^{P_k} h_{k,p}\, \boldsymbol{x}_k(t-\tau_{k,p})\, \mathrm{e}^{j2\pi\nu_{k,p}(t-\tau_{k,p})} + \boldsymbol{w}(t)\,, \quad (1)$$

where P_k is the number of propagation paths for the signal of user k, while $h_{k,p}$, $\tau_{k,p}$ and $\nu_{k,p}$ represent the channel gain, the delay and the Doppler shift of the p-th path, respectively. We assume every channel path to be subject to Rayleigh fading, hence $h_{k,p}$ are sampled from the complex Gaussian distribution $\mathcal{CN}\,(0, 1/P_k)$. Each entry of the noise vector $\boldsymbol{w}(t)$ is an i.i.d. realization of $\mathcal{CN}(0, \sigma^2)$. We denote the maximum delay and Doppler shift as $\tau_{\max}$ and $\nu_{\max}$. The symbol time T_s is given as the reciprocal of the bandwidth B, while $T_f = n_p T_s$ is the preamble frame duration. In this work, we assume $\tau_{k,p} = i\,T_s$ for $i \in \{0, 1, \ldots, \tau_{\max}\}$ and $\nu_{k,p} = j\,\frac{1}{T_f}$ for $j \in \{-\nu_{\max}{+}1, \ldots, \nu_{\max}\}$, i.e., that DD shifts are integer multiples of T_s and $1/T_f$. While fractional DD shifts can be estimated through additional signal processing operations (see, e.g., [22] and reference therein), they can also be considered as multiple on-grid channel components at the price of reduced channel sparsity. The explicit incorporation of off-grid DD shifts in our system model falls outside the scope of this paper and is left for future work. The decoder's task is to identify the unordered list $D(\boldsymbol{y})$ containing the K_a messages transmitted by the active users. The per-user probability of error (PUPE) P_e is defined as

$$P_e = \frac{1}{K_a} \sum_{k=1}^{Ka} \mathbb{P}[\boldsymbol{x}_k \notin D(\boldsymbol{y})]\,.$$

The system's performance is computed in terms of energy efficiency, and thus, the relevant metric is the minimum energy per bit $E_b/N_0 = nP/(\sigma^2 b)$ required to achieve a target error probability P_e.

A. Transmitter

In this section, we describe the transmitter architecture with reference to Fig. 1. The message to be transmitted is split in two parts of b_p and b_c bits each, so that $b = b_p + b_c$ and $b_p < b_c$. The vectors $\boldsymbol{b}_p \in \{0,1\}^{b_p}$ and $\boldsymbol{b}_c \in \{0,1\}^{b_c}$ refer to the two message parts chosen by a generic user. Following the strategies of [6] and [7], the two message parts are encoded with different procedures. The resulting coded symbols are then transmitted on successive orthogonal resources so that the two do not interfere with each other.

The first b_p bits are used to index a preamble of length n_p. The mapping between bits and preambles is bijective. Each preamble symbol is i.i.d. and drawn from the distribution $\mathcal{CN}(0, 1/n_p)$. The set of preambles constitutes the columns of the matrix $\boldsymbol{A} \in \mathbb{C}^{n_p \times 2^{b_p}}$, which is called *sensing matrix*. The preamble set (hence the sensing matrix $\boldsymbol{A}$) is kept fixed once it has been designed, and is known to all users and the receiver. Once the transmitting user has chosen the preamble, such preamble is used to fill column-wise the matrix $\boldsymbol{X}_p \in \mathbb{C}^{M_p \times N_p}$ where $M_p N_p = n_p$. As the symbols in $\boldsymbol{X}_p$ are in the DD domain, the OTFS modulator block converts them to the time domain. The modulator is implemented using the inverse discrete Zak transform (IDZT) as

$$\boldsymbol{x}_p = \mathrm{vec}(\boldsymbol{X}_p \boldsymbol{F}_{N_p}^H)\,,$$

where the $\mathrm{vec}(\cdot)$ operator vectorizes the argument matrix along its columns, $\boldsymbol{F}_N$ is the discrete Fourier transform (DFT) matrix of size N, and ^{H} is the Hermitian operator. The last operation concerning the preamble is the addition of a CP of length $\tau_{\max}$ in front of it. The result of the aforementioned processing steps is the vector $\boldsymbol{x}_p^{cp}$ of length $n_p + \tau_{\max}$ symbols.

The remaining b_c bits are processed by the blocks at the bottom of Fig. 1. First, the bit sequence $\boldsymbol{b}_c$ is encoded with the cyclic redundancy check (CRC)-aided polar encoder according to the 5G new radio (5G-NR) standard. The encoded bits are modulated using quadrature phase shift keying (QPSK), and the resulting vector $\boldsymbol{\mu}_c$ is padded with zeros to obtain $\boldsymbol{\mu}_c'$ of length n_c. At this point, an interleaver $\boldsymbol{\Pi}_i$ performs a pseudo-random permutation of $\boldsymbol{\mu}_c'$, which is uniquely determined by the seed $\boldsymbol{b}_p$. By doing so, the preamble is used as side information for the data encoder and will be exploited at the receiver to reverse the interleaving operation. The rationale of this operation is to minimize the multi-user interference (MUI) given that the interleaving patterns are independently chosen by each user. The interleaved vector $\boldsymbol{\Pi}_{\boldsymbol{b}_p}(\boldsymbol{\mu}_c')$ is then reshaped to fill column-wise the DD matrix $\boldsymbol{X}_c \in \mathbb{C}^{M_c \times N_c}$ with $M_c N_c = n_c$. The OTFS modulator converts $\boldsymbol{X}_c$ into its discrete time representation $\boldsymbol{x}_c = \mathrm{vec}(\boldsymbol{X}_c \boldsymbol{F}_{N_c}^H)$, and finally, a CP of length $\tau_{\max}$ is prepended to $\boldsymbol{x}_c$ to obtain $\boldsymbol{x}_c^{cp}$.

The baseband representation of the overall transmitted signal by a generic user is given by $\boldsymbol{x} = [\boldsymbol{x}_p^{cp}, \boldsymbol{x}_c^{cp}] \in \mathbb{C}^n$. The total number of complex degrees of freedom of $\boldsymbol{x}$ is given by $n = n_b + n_c + 2\tau_{\max}$.

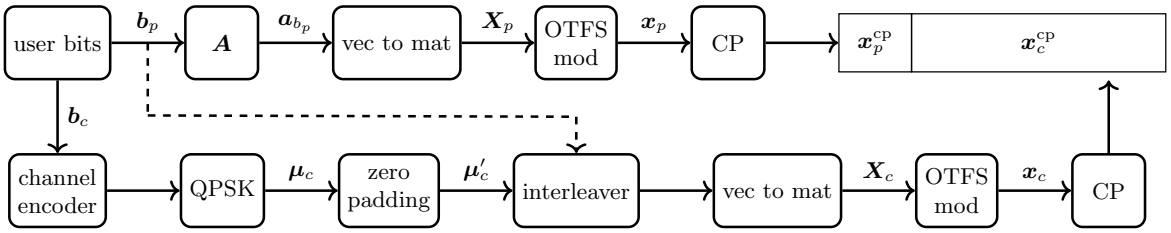

Fig. 1. Transmission scheme

B. Receiver

The K_a active users concurrently transmit over the same resources. Nevertheless, as shown in Eq. (1), the transmitted signals face different channels and will arrive at the receiver with different DD offsets, multiplicity, and complex gains. To retrieve the transmitted messages, the receiver needs to detect the number of active users and estimate their respective channels so that the received signals can be equalized and decoded. The preamble and data bits are estimated sequentially using different techniques. The continuous-time signal at the output of the channel is converted to baseband and sampled to obtain $\boldsymbol{y}$ as in Eq. (1). The receiver extracts the vectors $\boldsymbol{y}_p^{cp}$ and $\boldsymbol{y}_c^{cp}$ from $\boldsymbol{y}$ by taking the first $n_p + \tau_{\max}$ and the subsequent $n_c + \tau_{\max}$ complex symbols.

1) Compressed sensing (CS) preamble decoder: From the signal $\boldsymbol{y}_p^{cp}$, we remove the CP to obtain $\boldsymbol{y}_p$. The preamble decoder has the objective to estimate the active preamble set, denoted as $\mathcal{L}_p$, together with the channel parameters of all active users. This task can be seen through the lens of CS: the receiver must understand which columns of the sensing matrix are active by observing a noisy version of their superposition. In the case of GMAC or static fading, the sensing matrix observed by the receiver is exactly $\boldsymbol{A}$. When we consider a doubly-selective channel, instead, each preamble undergoes a channel with different delays and Doppler shifts. Their effect can be directly included in $\boldsymbol{A}$ by expanding the columns and including all possible shifted versions of each preamble. In the expanded sensing matrix, denoted as $\boldsymbol{A}_{\text{exp}}$ and of dimension $n_p \times \left(2^{b_p}\left(\tau_{\max}+1\right)2\nu_{\max}\right)$, each preamble will be found multiple times, once for each DD combination. The column of $\boldsymbol{A}_{\text{exp}}$ related to the i-th preamble and a (τ, ν) DD shift is

$$\boldsymbol{a}_i^{\tau,\nu} = (\mathbf{F}_{N_p} \otimes \mathbf{I}_{M_p})(\mathrm{e}^{-j\frac{2\pi}{N_p M_p}\nu\tau}\boldsymbol{\Delta}^{\nu}\boldsymbol{\pi}^{\tau})(\mathbf{F}_{N_p}^H \otimes \mathbf{I}_{M_p})\boldsymbol{a}_i\,,$$

where $\mathbf{I}_N$ is the identity matrix of size N, $\otimes$ is the Kronecker product, $\boldsymbol{\Delta}^{k_i} = \mathrm{diag}\left[\mathrm{e}^{\frac{j2\pi}{N_p M_p}\nu\cdot(0)}, \ldots, \mathrm{e}^{\frac{j2\pi}{N_p M_p}\nu\cdot(N_p M_p-1)}\right]$ and $\boldsymbol{\pi}$ is the cyclic shift matrix of size $N_p M_p \times N_p M_p$

$$\boldsymbol{\pi} = \begin{bmatrix} 0 & \cdots & 0 & 1 \\ 1 & \cdots & 0 & 0 \\ \vdots & \ddots & \vdots & \vdots \\ 0 & \cdots & 1 & 0 \end{bmatrix}.$$

The vector $\boldsymbol{a}_i^{\tau,d}$ can be interpreted as the vectorized DD signal seen at the receiver after the reception of the preamble $\boldsymbol{a}_i$ over a single tap channel with delay τ, Doppler ν and gain $h = 1$.

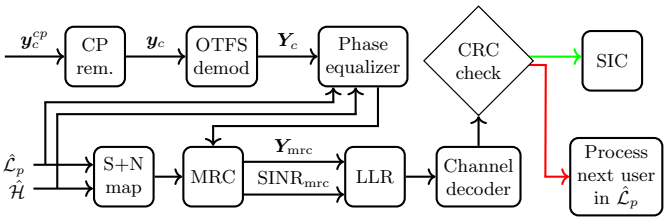

Fig. 2. Receiver scheme for data decoding.

Many algorithms are available in the literature to deal with the considered noisy CS decoding problem. Here we resort to approximate message passing (AMP) [23]. The input of the CS decoder is the measurement vector $\boldsymbol{y}_p^{dd} = (\mathbf{F}_{N_p} \otimes \mathbf{I}_{M_p})\boldsymbol{y_p}$, which represents the vectorized DD preamble signals observed by the receiver. Considering only the preamble part, the input-output relation in Eq. (1) can be rewritten as

$$\boldsymbol{y}_p^{dd} = \boldsymbol{A}_{\text{exp}}\,\boldsymbol{\varphi} + \boldsymbol{w}^{dd}\,,$$

where $\boldsymbol{\varphi} \in \mathbb{C}^{(2^{b_p}\,(\tau_{\max}+1)\,2\nu_{\max})\times 1}$ represents the sparse vector that the receiver aims to estimate and $\boldsymbol{w}^{dd}$ is the noise term in DD domain. In particular, the vector $\boldsymbol{\varphi}$ has $\sum_{k=1}^{K_a} P_k$ non-zero entries whose values are given by the $h_{k,p}$ channel coefficients. Through the AMP algorithm, we obtain the estimate $\hat{\boldsymbol{\varphi}}$ of $\boldsymbol{\varphi}$ starting from $\boldsymbol{y}_p^{dd}$ and $\boldsymbol{A}_{\text{exp}}$. Inspecting $\hat{\boldsymbol{\varphi}}$, we retrieve the estimated set of active preambles $\hat{\mathcal{L}}_p$ with their respective channel parameters composed of the number of propagation paths $\hat{P}_k$ and the complex attenuation, delay, and Doppler shift $(\hat{h}, \hat{\tau}, \hat{\nu})$ of each path. We call $\hat{\mathcal{H}}$ the set of estimated parameters describing the channels of all users, i.e., the $\hat{P}_k$ triplets of $(\hat{h}, \hat{\tau}, \hat{\nu})$. Depending on the prior statistical knowledge of $\boldsymbol{\varphi}$ available at the receiver, different denoisers can be adopted to enhance the performance of the AMP decoder [24]. Note that for small b_p and large active user population size K_a, the probability that two users select the same preamble becomes non-negligible. We discuss this issue in Sec. III.

2) Data decoder: The operations performed to estimate the vector $\boldsymbol{b}_c$ of each active user are shown in Fig. 2. After the CP removal, the DD representation of the signal $\boldsymbol{y}_c$ is computed as

$$\boldsymbol{Y}_c = \mathbf{F}_{N_c}\mathrm{vec}_{M_c N_c}^{-1}(\boldsymbol{y}_c)\,, \tag{2}$$

where $\mathrm{vec}_{ij}^{-1}(\cdot)$ reshapes the argument vector of length $(i \cdot j)$ into a matrix of size $i \times j$, filling the matrix column-wise. The operation in Eq. 2 is known as discrete Zak transform (DZT) and is performed by the OTFS demodulator block. The matrix $\boldsymbol{Y}_c$ contains multiple DD repetitions of the interleaved

source signal transmitted by each of the K_a users, where each repetition is shifted and scaled according to the channel parameters of the considered user.

At this point, the receiver employs a single-user decoding strategy, treating the MUI and inter-symbol interference (ISI) as Gaussian noise and triggering the successive interference cancellation (SIC) procedure whenever decoding succeeds. Exploiting the knowledge gained from the CS decoding phase (see Sec. II-B1) related to the active interleavers and their relative channel parameters, the receiver can estimate the aggregate signal strength on each DD symbol in the OTFS matrix $\boldsymbol{Y}_c$. By including also the noise power a signal plus noise map is constructed. The receiver's strategy is to use maximal-ratio combining (MRC) [25] at the symbol level among the channel echoes before attempting the decoding on the codeword. In particular, it extracts the selected interleaver from $\hat{\mathcal{L}}_p$ and the the corresponding channel parameters from $\hat{\mathcal{H}}$. It then proceeds by recovering from $\boldsymbol{Y}_c$ the symbols corresponding to each multipath echo with the aim of coherently combining them to get an enhanced signal-to-interference-plus-noise ratio (SINR). Note that, before combining, the symbols corresponding to each echo in $\boldsymbol{Y}_c$ have to be shifted back, de-interleaved, and equalized since different DD shifts introduce systematic phase rotations. These phase rotations can be obtained by means of the DZT [13], by computing the discrete input-output relation in DD domain. This can be done by considering a simple single user channel with a unique propagation path with DD coordinates (τ, ν) and unit gain:

$$\boldsymbol{Y}[m,n] = \mathrm{e}^{\frac{j2\pi\nu}{MN}(m-\tau)}\boldsymbol{X}[(m-\tau)_M,(n-\nu)_N]\mathrm{e}^{\frac{j2\pi}{N}(n-\nu)\left\lfloor\frac{m-\tau}{M}\right\rfloor} \tag{3}$$

where $\boldsymbol{X} \in \mathbb{C}^{M\times N}$ denotes the DD representation of the transmitted signal. With the help of the signal plus noise map and the estimated channel coefficients, the receiver can create the combined observation of the codeword $\boldsymbol{Y}_{\mathrm{mrc}}$. This is obtained as the symbol-level weighted sum of the phase-corrected echoes according to their respective SINRs. Finally, the combined observation $\boldsymbol{Y}_{\mathrm{mrc}}$ and the corresponding SINR values are used to produce the codeword bits log-likelihood ratios (LLRs) that are given as input to the successive cancellation list (SCL) decoder [26]. The output of the channel decoder is considered correct whenever the CRC check is satisfied. In this case, the receiver triggers the SIC procedure and subtracts from $\boldsymbol{Y}_c$ all the detected echoes of the decoded signal. The iterative process continues until either all users in $\hat{\mathcal{L}}_p$ are successfully decoded or until the decoder is no longer able to decode any remaining message.

III. Numerical results

In Fig. 3, we show the performance of the AMP decoder in terms of miss detection probability, namely the ratio of undetected preambles over the transmitted ones, for a varying number of active users K_a, assuming a single-path channel with unit channel coefficient. We dedicate to the preamble transmission $n_p = 640$ complex channel uses, organized in an OTFS matrix with $M_p = 40$ and $N_p = 16$. Other system

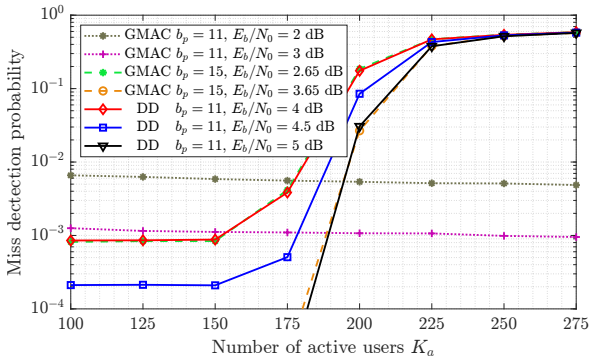

Fig. 3. Preamble miss detection probability versus the number of active users for different system and channel parameters.

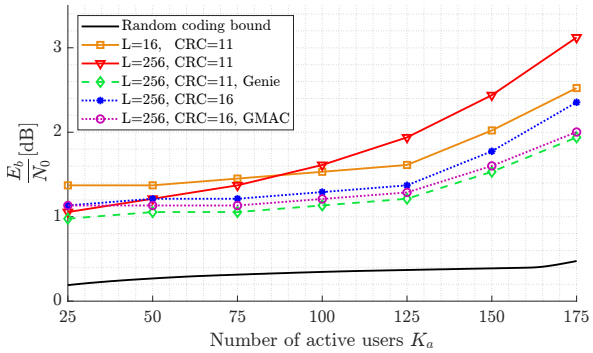

Fig. 4. Overall E_b/N_0 required to achieve $P_e = 0.05$ as a function of the number of active users assuming a single-path channel with unit gain.

parameters are $b_p = 11$, $\tau_{\max} = 3$ and $\nu_{\max} = 2$, hence, the expanded sensing matrix at the receiver $\boldsymbol{A}_{\exp}$ has dimensions 640×2^{15}. A preamble is considered undetected also if the receiver does not exactly recover its DD shift. A high recovery probability in the first phase is key for the overall system to work successfully as it provides key information for the data decoding phase. With the selected parameters, represented with the solid curves in Fig. 3, the recovery probability does not limit the overall system performance up to $K_a = 175$, having in mind a target $P_e = 0.05$. Other results are shown in the same figure for the case where $\tau_{\max} = 0$ and $\nu_{\max} = 0$, thus effectively resulting in the GMAC scenario. In this latter setting, it is possible to observe a smaller required E_b/N_0 to achieve similar error probabilities thanks to the less severe undersampling ratio (dotted curves). On the other hand, maintaining the same signal-to-noise ratio (SNR) and target miss detection probability, a greater number of bits could be embedded in the preamble signal (dashed curves). This phenomenon also demonstrates that $\boldsymbol{A}_{\exp}$ behaves as a true random i.i.d. matrix with Gaussian entries [23].

A first result related to the second protocol phase is shown in Fig. 4, where the required E_b/N_0 needed to achieve a target $P_e = 0.05$ is shown. Ideal decoding of the first phase is assumed, so that $\hat{\mathcal{L}}_p = \mathcal{L}_p$ and $\hat{\mathcal{H}} = \mathcal{H}$. The energy overhead due to the first protocol phase is already included in Fig. 4, and it is equal to an E_b/N_0 of 3 dB for the GMAC case and of 4 dB otherwise. The overall E_b/N_0 is computed as the

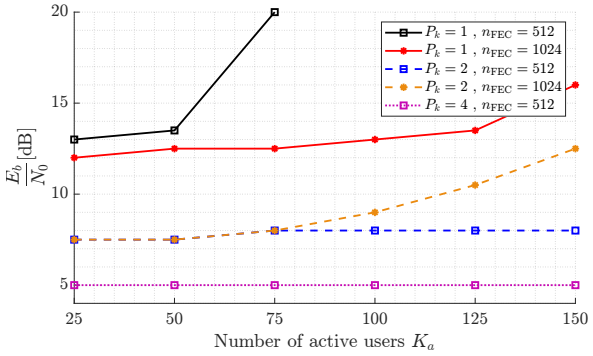

Fig. 5. E_b/N_0 needed in the the second protocol phase to achieve $P_e = 0.05$ in the presence of fading as a function of the number of active users for a varying number of multipath components P_k and code block-length n_{FEC}.

average, weighted according to number of information bits contained in each phase, between the preamble E_b/N_0 and the one required by the second protocol phase to reach the target P_e. The CPs are not counted into the energy budget. The additional simulation parameters are $M_c = 115$, $N_c = 128$, $b_c = 89$ and the considered channel is the same as the one with DD shifts in the previous experiment. The employed polar code has block-length $n_{\mathrm{FEC}} = 512$ and it takes as input $\boldsymbol{b}_c$ together with additional CRC bits. Here we describe the tradeoff between list size and CRC length. Large values of the list size enhance the error correction performance of the code. However, larger lists also lead to more undetected errors that can only be compensated with stronger CRCs. In Fig. 4, we report with solid lines the performance of the scheme when considering 11-bits CRC, list sizes 16, 256, and 256 with ideal error detection (denoted with the *Genie* label). We see that, for the case $L = 256$, better performance is achieved when the number of users is low, while the $L = 16$ case shows better performance when the number of active users increases, i.e., for $K_a \geq 125$. This phenomenon can be explained by the fact that undetected errors are particularly detrimental when SIC is employed. In fact, if a codeword is erroneously marked as correctly decoded, SIC is triggered, causing the introduction of additional interference that the receiver will not be able to remove later on. To enable the use of bigger lists, it is necessary to increase the error detection capability of the overall code by increasing the number of CRC bits. The performance of the scheme with $L = 256$ and a longer 16-bits CRC are also shown in Fig. 4. Thanks to the longer CRC, the undetected errors are strongly reduced. Nevertheless, it is worth noting that even this minor increase in code rate can lead to reduced error protection, which is the limiting factor for small K_a. Both dotted curves in Fig. 4 adopt the same polar encoder. Still, the GMAC performance are better due to the reduced preamble energy penalty and a slightly lower code rate due to $b_c = 85$.

In Fig. 5, the protocol performance is shown in the presence of the fading model described in Sec. II. We consider genie-aided error detection, meaning that no undetected errors occur. Assuming $P_k = 1$ for all active users, the scheme with $n_{\mathrm{FEC}} = 512$ and 16-bits CRC requires large E_b/N_0 values due to the too high outage probability, meaning that when the magnitude of the channel gain is too small, the decoder is not able to retrieve the transmitted codeword even in absence of MUI. A reduction in code rate enables a much better scaling of the scheme for a growing number of active users. When instead considering, $P_k \geq 2$ for each user, the outage probability becomes much smaller, and the MRC enables the exploitation of *multi-path diversity* thus rendering feasible the application of the higher rate polar code. This effect demonstrates the potential gain related to the capability of resolving and recombining the multipath echoes. Overall, while a growing number of multipath components renders the preamble estimation more difficult, it could result in better achievable performance of the scheme over fading channels.

In each of the protocol phases, we generate a signal in DD and then we convert it to the time domain by means of the OTFS modulator. Processing the signals in the DD domain allows us to cope with the double selectivity of the considered channel. When the channel DD spread is well confined inside an OTFS matrix, satisfying the crystallization condition [12], we have that all symbols within the OTFS matrix will experience the same channel up to some phase rotations that can be easily accounted for, see Eq. (3). This stationary behavior is in stark contrast with other multi-carrier schemes like OFDM, where each subcarrier experiences different gains and SNRs.

For the two-step approach, some discussion related to the use of the DD channel estimate among the different protocol phases should be made. In the proposed scheme, we exploit the preamble sequences, transmitted for each user within $\boldsymbol{X}_p$, to estimate the channels. The obtained channel estimate is then exploited to equalize the signal $\boldsymbol{Y}_c$ related to the second protocol phase. In the OTFS literature, channel estimation is typically done on a per-frame basis. Nevertheless, it is important to note that when two DD signals are transmitted sequentially, the channel variations acting on the two are not arbitrary. In particular, the DD channel representation enables a geometrical interpretation of the scene, where the DD coordinates of each path are related to the position and speed of a specific scatterer present in the scene. These attributes are, in general, slowly changing and could be considered approximately constant for a long time interval [13]–[15]. In this study, we consider a constant DD channel representation that spans both phases. Nevertheless, it is worth noting that, due to the presence of Doppler shifts, the considered input-output relation in Eq. (1) has the effect of a fast-varying frequency-selective channel, and is thus more general than the commonly adopted quasi-static fading model.

To avoid interference between $\boldsymbol{x}_p$ and $\boldsymbol{x}_c$, a CP is used in front of the latter signal. This choice, together with the fact that the two signals have different lengths and thus different sizes of the DD matrices, requires to apply some minor adjustments of the channel estimates derived in the first phase when exploited in the second one. While the delay resolution is proportional to the bandwidth B, which remains unchanged between the two phases, the Doppler resolution is proportional to the signal duration of each phase, and this can be easily

accounted for. The time duration of $\boldsymbol{x}_c$ equals αT_f with $\alpha \in \mathbb{R}$, and thus when the receiver estimates a Doppler-induced shift of ν_p bins within the DD preamble matrix, that same shift will be of $\nu_c = \alpha\nu_p$ in the following OTFS matrix. In general we have that $\frac{\nu_p}{T_f} = \frac{\nu_c}{\alpha T_f}$ and the system can be designed so that $\alpha \in \mathbb{N}$. An additional adjustment has to be applied to each complex gain $h_{k,p}$ to account for the total phase rotation that accumulates during the CP transmission due to the potential presence of a Doppler contribution.

In [19] an ad-hoc AMP denoiser for fractional DD channel has been recently developed, showing promising performance even in this more challenging setting. Note that fractional component can be seen as multiple integer ones, and thus the MRC principle can still be effectively used. Therefore, with some minor adjustment, the proposed scheme could also be used in the non-idealized scenario of fractional DD shifts.

Depending on the number of bits dedicated to the preamble and the number of active users K_a, the probability of preamble collisions may become non-negligible. Different from the GMAC setting, the user-specific channel effects, such as DD shifts and their related power profile, could be exploited to separate the contributions of the colliding users. In general, relying heavily on such an approach might not always be effective since colliding users might have too similar or indistinguishable channels. In general, it would be better to avoid preamble collision in the first place by increasing b_p. The limit of this latter solution is the convergence of the CS decoder, which, in the case of AMP, can be predicted by state evolution [23]. There is thus a tension between the number of preambles, driven by b_p, and the maximum channel DD spread that we are able to support. To mitigate this phenomenon one could increase the preamble length at the cost of reduced number of channel uses for the second protocol phase. Therefore, this latter choice trades a growing preamble set for a higher MUI in the second protocol phase.

IV. Conclusions

In this paper, we consider the problem of UMAC in the presence of doubly-dispersive channels. We propose and discuss the use of DD signal transmission based on multi-frame OTFS modulation as a key component for the construction of a grant-free multi-user scheme. Several design aspects are discussed and numerical results demonstrates that the proposed scheme shows competitive performance in the presence of residual time-frequency offsets. Furthermore, in the presence of multiple propagation paths, multipath diversity can be effectively exploited to combat the impact of fading. Further studies are needed to fully assess the scheme capabilities by considering the impact of imperfect channel estimation, fractional shifts and preamble collisions.

References

[1] D. C. Nguyen, M. Ding, P. N. Pathirana, A. Seneviratne, J. Li, D. Niyato, O. Dobre, and H. V. Poor, "6G Internet of Things: A comprehensive survey," *IEEE Internet Things J.*, vol. 9, no. 1, pp. 359–383, 2021.

[2] G. Liva and Y. Polyanskiy, "Unsourced multiple access: A coding paradigm for massive random access," *Proc. IEEE*, vol. 112, no. 9, pp. 1214–1229, 2024.

[3] Y. Polyanskiy, "A perspective on massive random-access," in *Proc. IEEE Int. Symp. Inf. Theory (ISIT)*, 2017, pp. 2523–2527.

[4] A. Fengler, P. Jung, and G. Caire, "SPARCs for unsourced random access," *IEEE Trans. Inf. Theory*, vol. 67, no. 10, pp. 6894–6915, 2021.

[5] A. Decurninge, I. Land, and M. Guillaud, "Tensor-based modulation for unsourced massive random access," *IEEE Wireless Commun. Lett.*, vol. 10, no. 3, pp. 552–556, 2021.

[6] A. K. Pradhan, V. K. Amalladinne, A. Vem, K. R. Narayanan, and J.-F. Chamberland, "Sparse IDMA: A joint graph-based coding scheme for unsourced random access," *IEEE Trans. Commun.*, vol. 70, no. 11, pp. 7124–7133, 2022.

[7] M. Ozates, M. Kazemi, and T. M. Duman, "Unsourced random access using odma and polar codes," *IEEE Commun. Lett.*, vol. 13, no. 4, pp. 1044–1047, 2024.

[8] R. Schiavone, G. Liva, and R. Garello, "Design and performance of enhanced spread spectrum aloha for unsourced multiple access," *IEEE Commun. Lett.*, vol. 28, no. 8, pp. 1790–1794, 2024.

[9] M. Gkagkos, K. R. Narayanan, J.-F. Chamberland, and C. N. Georghiades, "FASURA: A scheme for quasi-static fading unsourced random access channels," *IEEE Trans. Commun.*, vol. 71, no. 11, pp. 6391–6401, 2023.

[10] Y. Hu, D. Wang, X. Xia, J. Li, and P. Zhu, "Unsourced random access for mmwave massive MIMO-OFDM over doubly-selective channel," *IEEE Trans. Veh. Technol.*, pp. 1–6, 2025.

[11] Z. Wei, W. Yuan, S. Li, J. Yuan, G. Bharatula, R. Hadani, and L. Hanzo, "Orthogonal time-frequency space modulation: A promising next-generation waveform," *IEEE Wireless Commun.*, vol. 28, no. 4, pp. 136–144, 2021.

[12] S. K. Mohammed, R. Hadani, A. Chockalingam, and R. Calderbank, "OTFS—a mathematical foundation for communication and radar sensing in the delay-Doppler domain," *IEEE BITS Inf. Theory Mag.*, vol. 2, no. 2, pp. 36–55, 2022.

[13] T. T. Yi Hong and E. Viterbo, *Delay-Doppler Communications Principles and Applications*. Elsevier, 2022.

[14] F. Hlawatsch and G. Matz, *Wireless Communications Over Rapidly Time-Varying Channels*, 1st ed. USA: Academic Press, Inc., 2011.

[15] R. Hadani, S. Rakib, M. Tsatsanis, A. Monk, A. J. Goldsmith, A. F. Molisch, and R. Calderbank, "Orthogonal time frequency space modulation," in *Proc. IEEE WCNC*, 2017, pp. 1–6.

[16] A. K. Sinha, S. K. Mohammed, P. Raviteja, Y. Hong, and E. Viterbo, "OTFS based random access preamble transmission for high mobility scenarios," *IEEE Trans. Veh. Technol.*, vol. 69, no. 12, pp. 15 078–15 094, 2020.

[17] A. Mirri, V. Khammammetti, B. Dabak, E. Paolini, K. Narayanan, and R. Calderbank, "Zak-OTFS based coded random access for uplink mmtc," *arXiv: 2507.22013*, 2025.

[18] S. R. Mattu, I. A. Khan, V. Khammammetti, B. Dabak, S. K. Mohammed, K. Narayanan, and R. Calderbank, "Delay-Doppler signal processing with Zadoff-Chu sequences," *arXiv: 2412.04295*, 2024.

[19] A. Mirri, V. T. Kunde, B. Dabak, E. Paolini, and J.-F. Chamberland, "Approximate message passing for multi-preamble detection in OTFS random access," *arXiv: 2509.03980*, 2025.

[20] L. Ping, L. Liu, K. Wu, and W. Leung, "Interleave division multiple-access," *IEEE Trans. Wireless Commun.*, vol. 5, no. 4, pp. 938–947, 2006.

[21] P. Agostini, J.-F. Chamberland, F. Clazzer, J. Dommel, G. Liva, A. Munari, K. Narayanan, Y. Polyanskiy, S. Stanczak, and Z. Utkovski, "Enhancements to the 5G-NR 2-step RACH: an unsourced multiple access perspective," in *2024 IEEE Conference on Standards for Communications and Networking (CSCN)*, 2024, pp. 32–35.

[22] Q. Wang, Y. Liang, Z. Zhang, and P. Fan, "2D off-grid decomposition and sbl combination for OTFS channel estimation," *IEEE Trans. Wireless Commun.*, vol. 22, no. 5, pp. 3084–3098, 2023.

[23] D. L. Donoho, A. Maleki, and A. Montanari, "Message-passing algorithms for compressed sensing," *Proceedings of the National Academy of Sciences*, vol. 106, no. 45, pp. 18 914–18 919, 2009.

[24] L. Liu, E. G. Larsson, W. Yu, P. Popovski, C. Stefanovic, and E. de Carvalho, "Sparse signal processing for grant-free massive connectivity: A future paradigm for random access protocols in the Internet of Things," *IEEE Signal Process. Mag.*, vol. 35, no. 5, pp. 88–99, 2018.

[25] D. Brennan, "Linear diversity combining techniques," *Proc. IEEE*, vol. 91, no. 2, pp. 331–356, 2003.

[26] I. Tal and A. Vardy, "List decoding of polar codes," *IEEE Trans. Inf. Theory*, vol. 61, no. 5, pp. 2213–2226, 2015.